Maximum flux density of the gyrosynchrotron spectrum in a nonuniform source *

Ai-Hua Zhou[1], Rong-Chuan Wang[1] and Cheng-Wen Shao[1,2]

[1] Purple Mountain Observatory, Chinese Academy of Sciences, Nanjing 210008, China;
   zhouah@pmo.ac.cn
[2] Graduate University of Chinese Academy of Sciences, Beijing 100049, China

Abstract The maximum flux density of a gyrosynchrotron radiation spectrum in a magnetic diploe model with self absorption and gyroresonance is calculated. Our calculations show that the maximum flux density of the gyrosynchrotron spectrum increases with increasing low-energy cutoff, number density, input depth of energetic electrons, magnetic field strength and viewing angle, and with decreasing energy spectral index of energetic electrons, number density and temperature of thermal electrons. It is found that there are linear correlations between the logarithms of the maximum flux density and the above eight parameters with correlation coefficients higher than 0.91 and fit accuracies better than 10%. The maximum flux density could be a good indicator of the changes of these source parameters. In addition, we find that there are very good positive linear correlations between the logarithms of the maximum flux density and peak frequency when the above former five parameters vary respectively. Their linear correlation coefficients are higher than 0.90 and the fit accuracies are better than 0.5%.

Key words: Sun: flare — Sun: radio emission — Sun: maximum flux

1 INTRODUCTION

Radio emission from solar flares offers a number of unique diagnostic tools to address long-standing questions about energy release, plasma heating, particle acceleration and particle transport in magnetized plasma. At millimeter and centimeter wavelengths, i.e., the microwave (MW) wavelengths, incoherent gyrosynchrotron emission from energetic electrons plays a dominant role. These electrons carry a significant fraction of the energy released during the impulsive phase of flares.

A lot of effort has been done to try to answer the above questions. For example, the relations between the electron energy spectral index and the gyrosynchrotron spectral index were established to study particle acceleration (Dulk & Marsh 1982; Kucera et al. 1994; Zhou et al. 1998; Zhou, Huang & Wang 1999). The coronal magnetic fields and energy cutoffs of energetic electrons were estimated on the MW burst spectrum (e.g., Batchelor, Benz & Diehl 1984; Gary 1985; Bastian & Gary 1992; Lim et al. 1992; Zhou & Karicky 1994; Huang & Zhou 2000; Holman 2003; Fleishman & Melnikov 2003; Zhou, Su & Huang 2005; Huang et al. 2005; Huang 2006). In most of these studies, however, they usually assume a uniform magnetic field model, or ignore the gyroresonance or self absorption. We note that although it is valuable for the above studies to achieve a better understanding of general characteristics of the gyrosynchrotron spectrum, the homogeneous source assumption would, in general, deviate from reality.

For the case of an inhomogeneous source, several authors (e.g., Takakura & Scalise 1970; Takakura 1972; Alissandrakis & Preka-Paradema 1984; Klein & Trottet 1984) computed the gyrosynchrotron radiation in an attempt to discuss its spectral or spatial brightness distribution, but none of these studies further considered the influence of various parameters of burst source on the gyrosynchrotron spectrum. Recently, we comprehensively investigated the influence of these parameters of burst source on the peak frequency of a gyrosynchrotron spectrum and gave some applications (Zhou & Li 2007; Zhou, Li & Wang 2008).

The goal of this paper is to further reveal the proper effects of various burst source parameters on the maximum flux density, i.e., the peak flux density at peak frequency of the gyrosynchrotron spectrum. The computational model of a gyrosynchrotron spectrum is described in Section 2, the effects of various physical parameters on the maximum flux density of the gyrosynchrotron spectrum and the linear fits of the maximum flux density are calculated in Section 3. The correlations between the maximum flux and the peak frequency are obtained when some physical parameters vary in Section 4. The discussion and conclusions are given in Sections 5 and 6, respectively.

2 THE COMPUTATIONAL MODEL

Based on the general equation of radiative transfer, the radio flux density of gyrosynchrotron radiation is (Dulk & Marsh 1982)

$$S_{\nu\mp} = \Omega \int_0^{\tau_{\nu\mp}} (\eta_{\nu\mp}/\kappa_{\nu\mp})e^{-t_{\nu\mp}}dt_{\nu\mp} \quad (\text{erg s}^{-1}\,\text{Hz}^{-1}\,\text{cm}^{-2}), \tag{1}$$

where Ω is the solid angle in units of steradian (Sr); η_ν and κ_ν are, respectively, the emission and absorption coefficients; and τ_ν is the optical depth. The subscripts $-$ and $+$ correspond to the extraordinary and ordinary modes, i.e., the X-mode and O-mode respectively. Flare observations in both MW and hard X-rays have shown that the energy distribution of these energetic electrons is well described by a power law. Thus, the number density of the accelerated electrons can be written in the form, $n(E) = GE^{-\delta}(\text{electrons cm}^{-3}\,\text{keV}^{-1})$, where G is related to N by the relation $G = (\delta - 1)E_0^{\delta-1}N$ and N is the number of energetic electrons per cubic centimeter with $E > E_0$ (keV).

The flux density in units of sfu in a magnetic dipole field case is (Zhou, Su & Huang 2004)

$$S_{\nu\mp} = \frac{\Omega G\pi\, e^2 d}{3c}(2.8 \times 10^6 B_0)^{1/3}\nu^{2/3} \times 10^{19} \int_{s_0}^{s_m} \zeta_{s\mp}s^{-2/3}e^{-\tau_{\nu\mp}(s)}ds \quad (\text{sfu}), \tag{2}$$

where

$$\zeta_{s\mp} = \frac{1}{2|\cos\theta|} \sum_{n>s\sin\theta}^{\infty} \int_{p_0}^{p_m} (a \pm b)^2(1+p^2)^{-1}(\sqrt{1+p^2}-1)^{-\delta}dp,$$

under the quasi-longitudinal propagation condition.

In the above expressions, θ is the viewing angle and $s(= \nu/\nu_B)$ is the harmonic number. d is the depth under the photosphere of the magnetic dipole. s_0 and s_m are, respectively, the harmonic numbers of the emissions from the lower boundary h_d (which reflects the input depth of the energetic electrons) and upper boundary h_u of the radio source for a given frequency ν. $\tau_{\nu\mp}(s)$ is the sum of the optical depths for the self absorption and gyroresonance absorption ($\tau_{\nu\mp}(s) = \tau_{\nu\mp}^{\text{self}} + \tau_{\nu\mp}^{\text{gyro}}$).

A set of typical parameters of a radio burst is selected for gyrosynchrotron spectral computations, including $\delta = 3$, $E_0 = 10\,\text{keV}$, $N = 10^5\,\text{cm}^{-3}$, $B_0 = 3000\,\text{G}$, $\theta = 60°$ and $h_d = 1.8 \times 10^9\,\text{cm}$. The appropriate change in the ranges of the parameters are selected (c.f. Stahli, Gary & Hurford 1989; Huang 2000; Gan et al. 2002; Holman 2003; Zhou, Su & Huang 2005; Huang 2006). The accuracy of the theoretical peak frequency ν_p reaches $\pm 0.1\,\text{GHz}$ in our numerical computations.

3 MAXIMUM FLUX DENSITY OF GYROSYNCHROTRON SPECTRUM

3.1 Energetic Electrons

The effects of the accelerated electron parameters on the gyrosynchrotron spectrum are computed in detail. The calculations show that a decrease in the energy spectral index can result in a great increase of the peak flux density at peak frequency, i.e., the maximum flux of the spectrum. For example, when the energy spectral index decreases from 10 to 1.2, the maximum flux increases from 5 to 174 000 sfu, i.e., it increases 33 000 times for the X-mode. Furthermore, there is a good linear fit between the logarithms of the peak flux and the energy spectral index in the 10–1.2 whole range. The fit results are given in Figure 1 (left panel) and Table 1, where γ and SD are the correlation coefficient and standard error deviation of the linear fit, respectively.
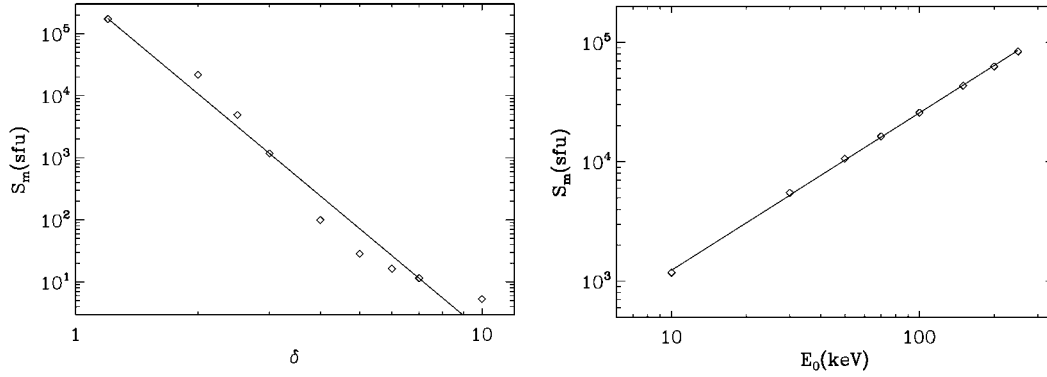
Fig. 1 Left panel is the linear fit between the logarithms of the maximum flux density and the energy spectral index of energetic electrons in the 1.2 to 10 range for the X-mode, right panel is same as the left one but between logarithms of the maximum flux density and the low-energy cutoff in the 10 to 250 keV range.

Table 1 Linear Fit Results of the Peak Flux

X	Y	Mode	a	b	γ	SD	SD(%)
$\log \delta$	$\log S_m$	X	5.68	-5.46	-0.98	0.288	10
$\log E_0$	$\log S_m$	X	1.78	1.32	~ 1	0.012	0.3
$\log N$	$\log S_m$	X	-0.172	0.654	~ 1	0.029	0.9
$\log h_d$	$\log S_m$	X	8.02	-0.536	~ -1	0.045	1.4
$\log B_0$	$\log S_m$	X	-1.30	1.26	~ 1	0.010	0.3
$\log \theta$	$\log S_m$	O	-0.745	2.03	0.98	0.104	4.2
$\log N_{\text{th}}$	$\log S_m$	X	3.67	-0.212	-0.91	0.060	3.7
$\log T_{\text{th}}$	$\log S_m$	X	5.63	-0.590	-0.93	0.089	5.3
E_0	S_m	X	-6.09×10^3	3.47×10^2	~ 1	2.37×10^3	7.6
h_d	S_m	X	2.88×10^3	-8.96×10^{-7}	-0.97	1.62×10^2	9.2
B_0	S_m	X	-2.13×10^2	0.481	~ 1	56.4	5.8

The effect of the high-energy cutoff of energetic electrons on the gyrosynchrotron spectrum is small and the peak frequency and the maximum flux density are relatively constant. However, the low-energy cutoff significantly affects the gyrosynchrotron spectrum, not only for the peak frequency, but also for the peak flux density. For example, when the low-energy cutoff increases from 10 to 250 keV, the maximum flux density increases about two orders of magnitude for the X-mode. Furthermore, there is also a good linear fit between the logarithms of the peak flux and the low-energy cutoff in the whole
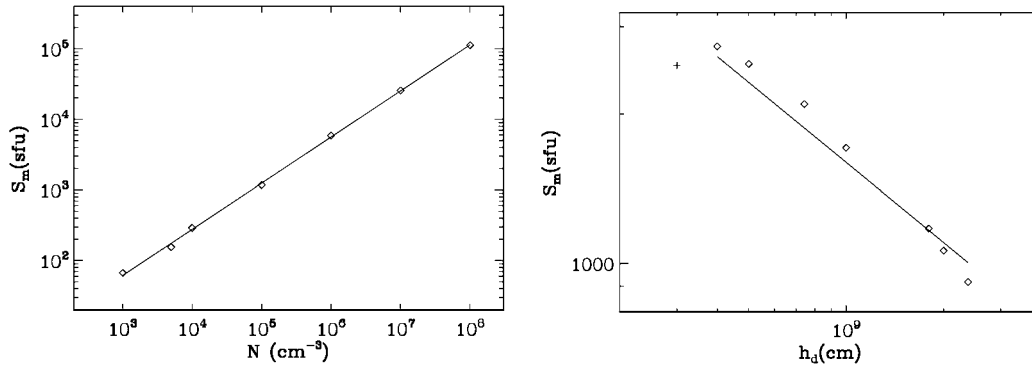
Fig. 2 Same as Fig. 1, but it is between the logarithms of the maximum flux density and the number density of energetic electrons in the 10^3 to 10^8 cm^{-3} range (left panel) and between the logarithms of the maximum flux density and lower boundary height of the burst source in the $(2.38 - 0.4) \times 10^9$ cm range (right panel).

range from 10 to 250 keV of low-energy cutoff. The fit result between the logarithms of the peak flux and the low-energy cutoff is given in Figure 1 (right panel).

The influence of the number density of energetic electrons on the maximum flux density of gyrosynchrotron spectrum is also very great. When the number density increases from 10^3 to 10^8 cm^{-3}, the maximum flux density increases from 67 to 113 000 sfu (about 1700 times) for the X-mode. There is also a good linear fit between the logarithms of the peak flux and the number density of energetic electrons (see Fig. 2).

3.2 Burst Source

It is shown from our study that the upper boundary height of a burst source only changes the distribution of flux density at the lower frequencies of the optically thick part, so the flux at the peak frequency does not depend on the upper boundary height of the burst source. However, it depends strongly on the lower boundary height of the burst source. When the lower boundary height decreases from 2.38×10^9 to 4×10^8 cm, the peak flux increases from 918 to 2740 sfu. Figure 2 (right panel) shows that there is also a good linear correlation between the logarithms of the peak flux and the lower boundary height in the $(2.38 - 0.4) \times 10^9$ cm range for the X-mode. However, when the lower boundary height decreases further from 4×10^8 cm, the peak flux begins to decrease (see the "+" symbol in Fig. 2), which results from the strong self absorption and gyroresonance absorption.

The numerical computations also show that when the magnetic field strength at the photosphere increases, the flux density obviously increases and the peak frequency shifts from lower to higher frequency. For example, when the photospheric magnetic field strength increases from 800 to 5000 G, the peak flux and the peak frequency increase, respectively, from 220 to 2300 sfu and from 3.4 to 18 GHz for the X-mode. This means that the increase in amplitude of the peak flux is less than that of the peak frequency, when the photospheric magnetic field strength increases. In addition, the peak flux density also increases with increasing viewing angle, i.e., it has an obvious radial effect. Here, we will give the impacts of magnetic field strength and viewing angle on the peak flux in Figure 3.

The gyrosynchrotron radiation also suffers absorption from thermal electrons in the burst source, i.e., gyroresonance absorption. So, thermal electron parameters might also affect the gyrosynchrotron spectrum due to the gyroresonance absorption. It is shown that the flux density of the optically thick part decreases with increasing number density and temperature of thermal electrons, which leads to the peak frequency shifts from the lower frequency to higher frequency with increasing density and temperature,
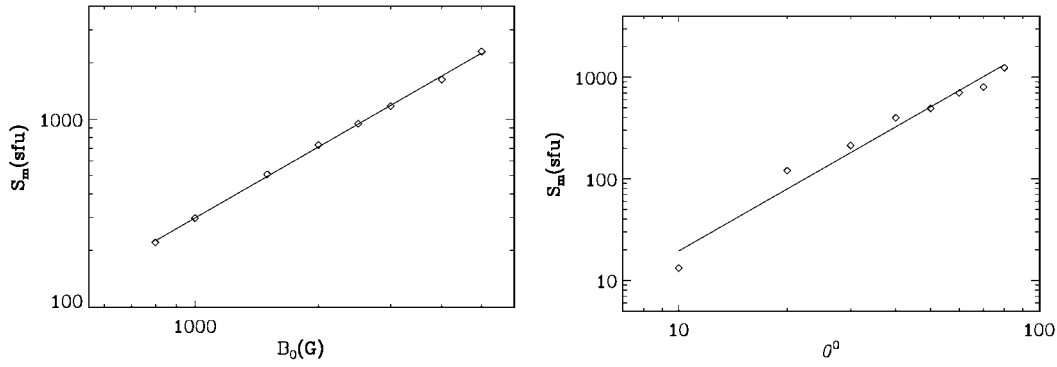
Fig. 3 Same as Fig. 1, but it is between the logarithms of the maximum flux density and the photospheric magnetic field strength in the 800 to 5000 G range for the X-mode (left panel) and between the maximum flux density and the viewing angle in the $10°$ to $80°$ range for the O-mode (right panel).
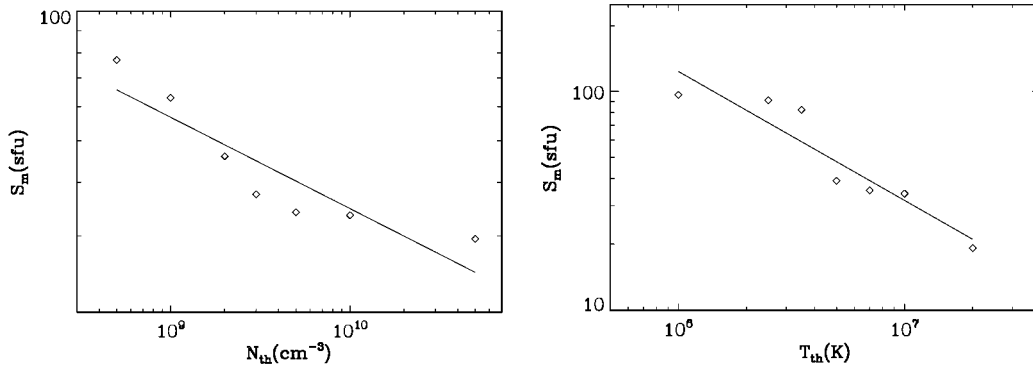
Fig. 4 Same as Fig. 1, but it is between the logarithms of the maximum flux density and the number density of thermal electrons in the 5×10^8 to 5×10^{10} cm^{-3} range (left panel) and between the logarithms of the maximum flux density and the temperature of thermal electrons in the 10^6 to 2×10^7 K range (right panel).

but only a little. For example, when the density and temperature increase, respectively, from 5×10^8 to 5×10^{10} cm^{-3} and 10^6 to 2×10^7 K, the peak frequency shifts, respectively, from 8 to 10 GHz and 8 to 10.5 GHz for the X-mode. Under the same conditions, however, the maximum flux obviously decreases with increasing density and temperature of thermal electrons. The decrement of the peak flux reaches 62% and 80% respectively. Furthermore, the decrease of the logarithm value of the peak flux is proportional to the increases in the logarithm values of the density and temperature of thermal electrons (see Fig. 4). The above fit results are also given in Table 1 for comparison.

4 CORRELATION BETWEEN THE PEAK FREQUENCY AND MAXIMUM FLUX DENSITY

Here, we will study the correlations between the peak frequency and the peak flux when the various burst parameters change. We find that when the low-energy cutoff, number density, lower boundary height of energetic electrons, the photospheric magnetic field strength and viewing angle vary, both the logarithms of the maximum flux density and peak frequency change proportionally. This means that
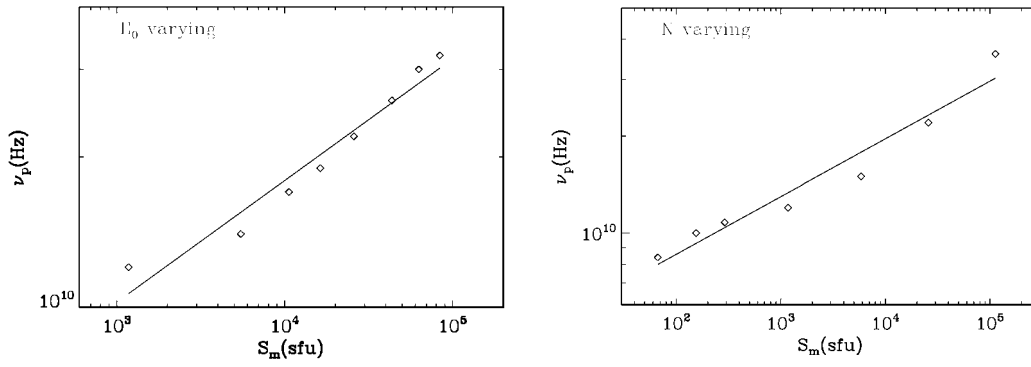
Fig. 5 Linear fit between the logarithms of the peak frequency and the maximum flux density when the low-energy cutoff E_0 changes in the 10 to 250 keV range (left panel) and the number density of energetic electrons N changes in the 10^3 to 10^8 cm^{-3} range for the X-mode (right panel).
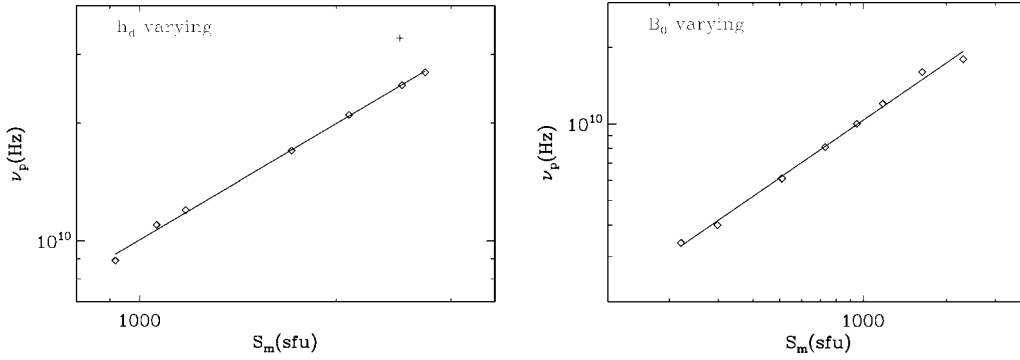
Fig. 6 Same as Fig. 5, but when the lower boundary height of burst source h_d changes in the $(2.38 - 0.4) \times 10^9$ cm range (left panel) and the photospheric magnetic field strength B_0 varies in the 800 to 5000 G range (right panel).

Table 2 Correction of the Peak Frequency and the Peak Flux

Variable	X	Y	mode	a	b	γ	SD	SD(%)
E_0	$\log S_m$	$\log \nu_p$	X	9.27	0.245	0.98	0.032	0.3
N	$\log S_m$	$\log \nu_p$	X	9.58	0.179	0.97	0.046	0.5
h_d	$\log S_m$	$\log \nu_p$	X	7.04	0.986	~ 1	0.009	0.1
B_0	$\log S_m$	$\log \nu_p$	X	7.76	0.752	~ 1	0.018	0.2
θ	$\log S_m$	$\log \nu_p$	O	9.58	0.144	0.90	0.042	0.4
E_0	S_m	ν_p	X	1.40×10^{10}	2.40×10^5	0.97	1.56×10^9	7.3
h_d	S_m	ν_p	X	3.48×10^8	9.78×10^6	~ 1	2.14×10^8	1.1
B_0	S_m	ν_p	X	2.43×10^9	7.45×10^6	0.98	8.82×10^8	9.1

there are linear correlations between the logarithms of the peak frequency and the peak flux. Figures 5–7 and Table 2 give their linear fit results between the logarithms of the peak frequency and the peak flux when the above five parameters vary, respectively.
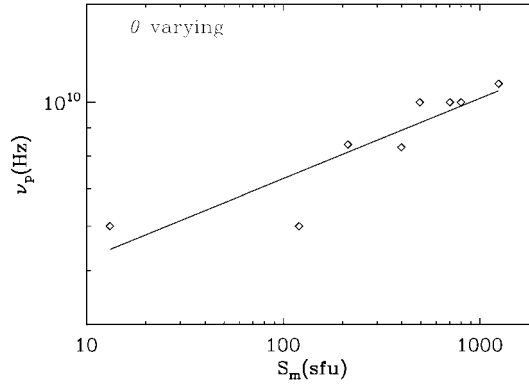
Fig. 7 Same as Fig. 5, but when the viewing angle θ varies in the $10°$ to $80°$ range for the O-mode.

However, there are no good linear fits between the logarithms of the the peak frequency and peak flux when the spectral index of energetic electrons, the number density and temperature of thermal electrons vary.

5 DISCUSSION

The peak flux density increases with the increases in the low-energy cutoff, number density, input depth of energetic electrons, photospheric magnetic field strength and viewing angle and with decreases in the energy spectral index of energetic electrons, number density and temperature of thermal electrons. The calculations show their linear correlation coefficients and their fit accuracies are, respectively, higher than 0.91 and better than 10% for the fit of $\log S_m$ (see Figs. 1–4 and Table 1). It is also found from our study that there is a good linear correlation between the peak flux S_m (sfu) and the low-energy cutoff E_0 (keV), lower boundary height of burst source h_d (cm) and photospheric magnetic field strength B_0 (G) respectively, i.e., they can also be expressed as simpler relations:

$$
\begin{aligned}
S_m &= -6090 + 347E_0 \pm 2371\,, \\
S_m &= 2880 - 8.96 \times 10^{-7} h_d \pm 162\,, \\
S_m &= -213 + 0.481B_0 \pm 56.4\,.
\end{aligned}
\tag{3}
$$

Their linear correlation coefficients and fit accuracies are, respectively, higher than 0.97 and better than 9.2 % for Equation (3) (see Figs. 8–9 and Table 1).

When the five variables, i.e., the low-energy cutoff, number density, input depth of energetic electrons, photospheric magnetic field strength and viewing angle vary, both the logarithms of the peak flux density and peak frequency change proportionally. Figures 5-7 and Table 2 also give their linear fit results between the logarithms of the peak frequency and the peak flux density. Their linear correlation coefficients and fit accuracies are, respectively, higher than 0.90 and better than 0.5%. We also find that there is a good linear correlation between the peak frequency ν_p (Hz) and the flux density S_m (sfu) when the low-energy cutoff E_0, lower boundary height of burst source h_d and photospheric magnetic field strength B_0 vary, they are:

$$
\begin{aligned}
\nu_p &= 1.40 \times 10^{10} + 2.40 \times 10^5 S_m \pm 1.56 \times 10^9 & (E_0 \text{ varying})\,, \\
\nu_p &= 3.48 \times 10^8 + 9.78 \times 10^6 S_m \pm 2.14 \times 10^8 & (h_d \text{ varying})\,, \\
\nu_p &= 2.43 \times 10^9 + 7.45 \times 10^6 S_m \pm 8.82 \times 10^8 & (B_0 \text{ varying})\,.
\end{aligned}
\tag{4}
$$

Their linear correlation coefficients and fit accuracies are, respectively, higher than 0.97 and better than 9.1% for Equation (4) (see Table 2).
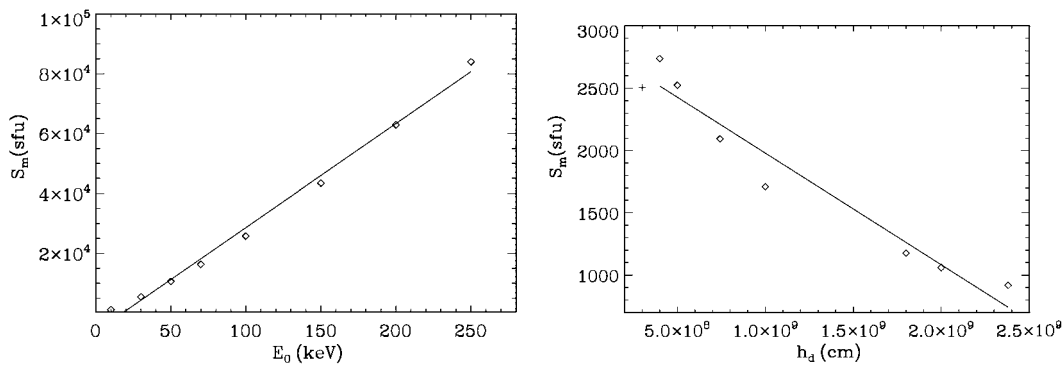
Fig. 8 Linear fit of the maximum flux density in the 10 to 250 keV range of the low-energy cutoff (left panel) and in the $(2.38 - 0.4) \times 10^9$ cm range of the lower boundary height of burst source (right panel) for the X-mode on the linear x and y-axes.
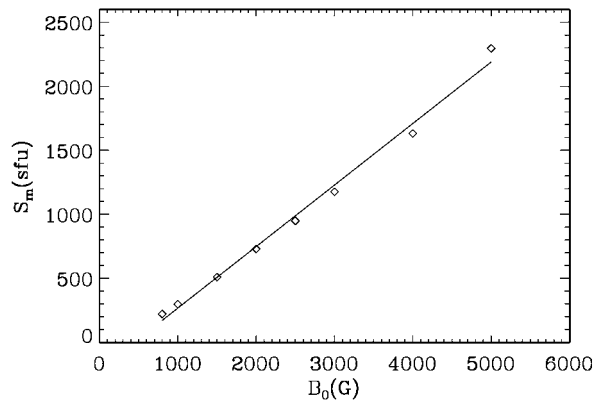
Fig. 9 Same as Fig. 8, but in the 800 to 5000 G range of the photospheric magnetic field strength.

It is shown from our studies that the maximum flux density varies with the changes of various parameters. The left panel of Figure 10 shows the change in amplitudes of the peak flux. It is found that when the electron energy spectral index decreases from 10 to 1.2, the maximum flux of the X-mode increases from 5 to 174 000 sfu for the X-mode, i.e., its increase exceeds more than four orders of magnitude. This means that the effect of electron energy spectral index on the peak flux is the most sensitive among these parameters. The next most sensitive parameter for the influence on the peak flux is the number density of energetic electrons. For example, when the number density increases from 10^3 to 10^8 (cm^{-3}), the maximum flux of the X-mode increases from 67 to 113 000 sfu, i.e., its increase exceeds more than three orders of magnitude. So, the peak flux could be a sensitive indicator of the electron acceleration. It was shown that the peak frequency also varies with the changes of various parameters. The right panel of Figure 10 gives the changes in the peak frequency to compare with the peak flux changes under the same conditions. Figure 10 (right panel) shows that when the magnetic field strength at the photosphere increases from 800 to 5000 G, the peak frequency can shift from 3.4 to 18 GHz for the X-mode. It means that the effect of the magnetic field strength on the peak frequency is the most sensitive among these parameters. Moreover, there is a very good linear correlation between the logarithms of the peak frequency and the photospheric magnetic field strength. Its linear correlation
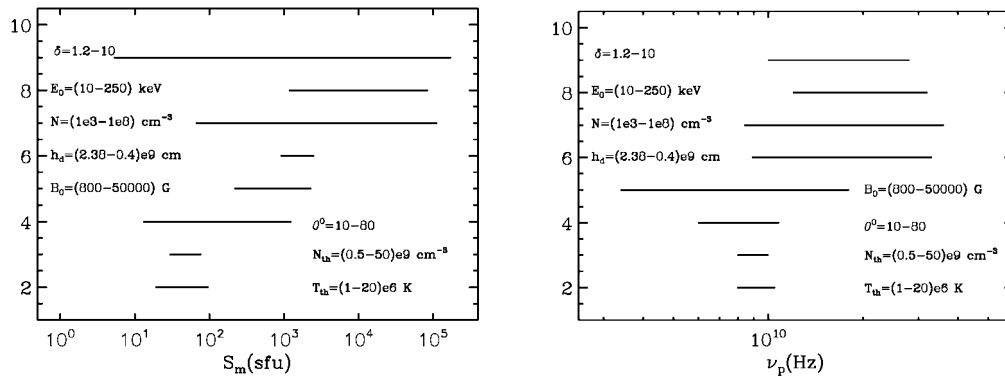
Fig. 10 Changes in ranges of the peak flux (left panel) and peak frequency (right panel) of gyrosynchrotron spectrum.

coefficient and fit accuracy reach, respectively, ~ 1 and 0.2% (Zhou, Li & Wang 2008). So, the peak frequency could be an ideal indicator of the magnetic field strength in burst regions.

Because the parameters might be rather different in different burst regions or during the evolution of a burst, the observational peak flux and peak frequency can vary over a very wide range.

6 CONCLUSIONS

The model computations which include self absorption and gyroresonance in the case of a nonuniform magnetic field show the effects of the electron parameters and the source parameters on the gyrosynchrotron spectrum to be rather essential. We discover that the maximum flux density of a gyrosynchrotron spectrum increases with increasing low-energy cutoff, number density, input depth of energetic electrons, magnetic field strength and viewing angle, and with decreasing energy spectral index of energetic electrons, number density and temperature of thermal electrons. It is found for the first time that there are linear correlations between the logarithms of the maximum flux density and the above eight parameters with correlation coefficients higher than 0.91 and fit accuracies better than 10%. The maximum flux density could be a good indicator of the changes of these source parameters.

Meanwhile, it is shown in the theory that there are also good linear correlations between the logarithms of the peak flux and peak frequency when the five parameters: the low-energy cutoff, number density, input depth of energetic electrons, magnetic field strength and viewing angle vary. Their linear correlation coefficients and fit accuracies are higher than 0.90 and better than 0.5%.

We also discover that when the energy spectral index of energetic electrons decreases from 10 to 1.2, the increase in the maximum flux can exceed four orders of magnitude. It means that the effect of electron energy spectral index on the peak flux is the most sensitive among these parameters. The second most sensitive parameter which influences the peak frequency is the number density of energetic electrons. The peak frequency also varies with the changes of various parameters. The effect of the magnetic field strength on the peak frequency is the most sensitive among these parameters. Therefore, the peak flux and peak frequency could be good indicators of the electron acceleration and the magnetic field strength of burst regions, respectively.

In this paper, for the first time, we have comprehensively explored the quantitative linear relations between the logarithms of the peak flux and the above eight source parameters and between the logarithms of the peak frequency and peak flux when the above former five parameters vary. Their linear correlation coefficients and linear fit accuracies are high. We think that these fit relations would be valuable for understanding the MW burst spectral observations and for the diagnostics of the physical parameters in a microwave burst source.

References

Alissandrakis, C. E., & Preka-Papadema, P. 1984, A&A, 139, 507
Bastian, T. S., & Gary, D. E. 1992, Solar Phys., 139, 357
Batchelor, D. A., Benz, A. O., & Wiehl, H. J. 1984, ApJ, 280, 879
Dulk, G. A., & Marsh, K. A. 1982, ApJ, 259, 350
Fleishman, G. D., & Melnikov, V. F. 2003, ApJ, 587, 823
Gan, W. Q., Li, Y. P. , Chang, J., et. al. 2002, Solar phys., 207, 137
Gary, D. E. 1985, ApJ, 297, 799
Holman, G. D. 2003, ApJ, 586, 606
Huang, G.-L. 2000, Solar Phys., 272, 325
Huang, G. 2006, ChJAA (Chin. J. Astron. Astrophys.), 6, 113
Huang, G. 2006, Solar Phys., 237, 173
Huang, G.-L., & Zhou, A.-H. 2000, New Astron., 4, 591
Huang, G., Zhou, A., Su, Y., et. al. 2005, New Astron., 10, 219
Klein, K. L., & Trottet, G. 1984, A&A, 141, 67
Kucera, T. A., Dulk, G. A., Gary, D. E., et al. 1994, ApJ, 433, 875
Lim, J., White, S. M., Kumdu, M. R., & Gary, D. E. 1992, Solar phys., 140, 343
Stahli, M., Gary, D. E., & Hurford, G. J. 1989, Solar Phys., 120, 351
Takakura, T., & Scalise, E. Jr. 1970, Solar Phys., 11, 434
Takakura, T. 1972, Solar Phys., 26, 151
Zhou, A.-H., & Karlisky, M. 1994, Solar Phys., 153, 441
Zhou, A.-H., & Li, J.-P. 2007, ChJAA (Chin. J. Astron. Astrophys.), 7, 487
Zhou, A.-H., Huang, G.-L., & Wang, X.-D. 1999, Solar Phys., 189, 345
Zhou, A.-H., Su, Y.-H., & Huang, G.-L. 2004, Chin. Phys. Lett., 21(10), 2067
Zhou, A. H., Su, Y. N., & Huang, G. L. 2005, Solar Phys., 226, 327
Zhou, A. H., Li, J. P., & Wang, X. D. 2008, Solar Phys., 247, 63
Zhou, A.-H., Ma, C.-Y., Zhang, J., et al. 1998, Solar Phys., 177, 427